

Functional Magnetic Resonance Imaging of Visual Object Construction and Shape Discrimination: Relations among Task, Hemispheric Lateralization, and Gender

Apostolos P. Georgopoulos^{1,2}, Kenneth Whang^{1,2},
Maria-Alexandra Georgopoulos^{1,2}, Georgios A. Tagaris^{1,2},
Bagrat Amirikian^{1,2}, Wolfgang Richter², Seong-Gi Kim², and
Kâmil Uğurbil²

Abstract

■ We studied the brain activation patterns in two visual image processing tasks requiring judgements on object construction (FIT task) or object sameness (SAME task). Eight right-handed healthy human subjects (four women and four men) performed the two tasks in a randomized block design while 5-mm, multislice functional images of the whole brain were acquired using a 4-tesla system using blood oxygenation dependent (BOLD) activation. Pairs of objects were picked randomly from a set of 25 oriented fragments of a square and presented to the subjects approximately every 5 sec. In the FIT task, subjects had to indicate, by pushing one of two buttons, whether the two fragments could match to form a perfect square, whereas in the SAME task they had to decide whether they were the same or not. In a control task, preceding and following each of the two tasks above, a single square was presented at the same rate and subjects pushed any of the two keys at random. Functional activation maps were constructed based on a combination of conservative criteria. The areas with activated pixels were identified using Talairach coordinates and anatomical landmarks, and the number of activated pixels was determined for each area. Altogether, 379 pixels were activated. The counts of activated pixels did not differ significantly between the two tasks or between the two genders. However, there were significantly more activated pixels in the left ($n = 218$) than the right side of the brain ($n = 161$).

Of the 379 activated pixels, 371 were located in the cerebral cortex. The Talairach coordinates of these pixels were analyzed with respect to their overall distribution in the two tasks. These distributions differed significantly between the two tasks. With respect to individual dimensions, the two tasks differed significantly in the anterior–posterior and superior–inferior distributions but not in the left–right (including mediolateral, within the left or right side) distribution. Specifically, the FIT distribution was, overall, more anterior and inferior than that of the SAME task.

A detailed analysis of the counts and spatial distributions of activated pixels was carried out for 15 brain areas (all in the cerebral cortex) in which a consistent activation (in ≥ 3 subjects) was observed ($n = 323$ activated pixels). We found the following. Except for the inferior temporal gyrus, which was activated exclusively in the FIT task, all other areas showed activation in both tasks but to different extents. Based on the extent of activation, areas fell within two distinct groups (FIT or SAME) depending on which pixel count (i.e., FIT or SAME) was greater. The FIT group consisted of the following areas, in decreasing FIT/SAME order (brackets indicate ties): GTi, GTs, GC, GFi, GFd, [GTm, GF], GO. The SAME group consisted of the following areas, in decreasing SAME/FIT order: GOi, LPs, Sca, GPrC, GPoC, [GFs, GFm]. These results indicate that there are distributed, graded, and partially overlapping patterns of activation during performance of the two tasks. We attribute these overlapping patterns of activation to the engagement of partially shared processes.

Activated pixels clustered to three types of clusters: FIT-only (111 pixels), SAME-only (97 pixels), and FIT + SAME (115 pixels). Pixels contained in FIT-only and SAME-only clusters were distributed approximately equally between the left and right hemispheres, whereas pixels in the SAME + FIT clusters were located mostly in the left hemisphere. With respect to gender, the left–right distribution of activated pixels was very similar in women and men for the SAME-only and FIT + SAME clusters but differed for the FIT-only case in which there was a prominent left side preponderance for women, in contrast to a right side preponderance for men. We conclude that (a) cortical mechanisms common for processing visual object construction and discrimination involve mostly the left hemisphere, (b) cortical mechanisms specific for these tasks engage both hemispheres, and (c) in object construction only, men engage predominantly the right hemisphere whereas women show a left-hemisphere preponderance. ■

INTRODUCTION

Visual images can be used for different purposes, depending on specific tasks. Visual processing tasks com-

¹Veterans Affairs Medical Center, Minnesota, ²University of Minnesota Medical School

prise, in turn, a large variety of operations, ranging from simple detection of visual stimuli to sophisticated discrimination or recognition of complex forms. In addition, the potentially multidimensional nature of visual stimuli, including form, color, and motion, all add substantially to the rich variety of behavioral tasks that can be employed to investigate visual functions at the behavioral and neural levels. Indeed, a wealth of information has accumulated on the brain mechanisms underlying various aspects of visual functions, based on studies of brain damaged subjects, recordings of single-cell activity in behaving monkeys, and, more recently, on functional neuroimaging studies in people. Among the latter studies, functional magnetic resonance imaging (fMRI) has become an increasingly prominent tool during the past several years. In the present study, we used BOLD fMRI imaging at high field (4 T) to investigate two specific visual functions, namely visual discrimination of simple line figures and visual construction of a square. Our approach was to use the same visual images for two different judgements in order to gain an insight into the brain mechanisms underlying the generation of these judgements under the same conditions of visuosensory stimulation. For that purpose, we used pairs of fragments of a square both as the discriminanda in the visual discrimination task (“Are they the same?”) and as the building blocks in the visual construction task (“Do they fit to make a perfect square?”). This latter task is of special interest, for it probes visuoconstructive functions extensively investigated in the neuropsychological literature. These investigations have dealt not only with determining the kinds of visuoconstructive deficits following brain damage but have also addressed questions of hemispheric lateralization of function and gender differences. Although these issues are somewhat controversial, it is commonly held that the right hemisphere plays a prominent role in visuoconstructive functions, especially so in men. Therefore, a specific objective of this study was to assess potential hemispheric asymmetries and gender differences in the visual discrimination and visual construction tasks used.

Finally, we wanted to examine in detail the spatial distribution patterns of activated pixels in order to gain an insight into the possibly differential or common involvement of specific brain areas in these tasks. For that purpose, we carried out a cluster analysis to determine whether pixels activated in a specific task form distinct clusters, or, to what extent they mix to form “common” clusters. Briefly, this analysis documented the existence of both separate, task-specific clusters, as well as combined-task, common clusters. The latter were located mostly in the left hemisphere whereas the former were about equally distributed in the two hemispheres. However, there was a substantial right-hemisphere preponderance of the visuoconstructive-specific pixels in men but not in women, in contrast to an equal left–right distribution of discrimination-specific pixels in the two genders.

RESULTS

Subjects performed at least 90%+ correct in both tasks. Altogether, 379 pixels showed changes from the control task.

Overall Analysis of Counts of Activated Pixels

Approximately equal numbers of pixels were activated in the two tasks ($n = 196$ for FIT versus 183 for SAME) whereas more pixels were activated on the left ($n = 218$) than the right side ($n = 161$), and more in men ($n = 207$) than in women ($n = 172$). The analysis of variance (see Methods) revealed only one statistically significant effect, namely the main effect of Side ($p = .0192$, F test); none of the main effects of Task or Gender, and none of the interaction terms were statistically significant.

Analysis of Spatial Distributions of Activated Pixels in Cerebral Cortex

Of a total of 379 activated pixels, 371 were located in the cerebral cortex (190 for the FIT and 181 for the SAME task). The Talairach coordinates of these pixels were analyzed with respect to their overall distribution, irrespective of the brain area to which they might belong. The location of each pixel in brain space was a vector with three coordinates (left–right, LR; anterior–posterior, AP; superior–inferior, SI). (In the LR distribution, the sign of a coordinate indicates the side whereas greater absolute values indicate increasing distance from the midsagittal plane.) Therefore, two 3-dimensional (3-D) distributions were available, one for the FIT and another for the SAME task. These distributions are shown in Figures 1 and 2 as 3-D vector plots. Statistically, they differed highly significantly (multivariate Hotelling’s T^2 test, $T^2 = 42.19$, $p < .0001$). A more detailed evaluation of the differences between these two distributions was obtained by analyzing their component distributions in the three coordinate planes. The corresponding frequency distributions are shown in Figures 3–5. The two tasks did not differ significantly with respect to the LR distributions (Figure 3) (Mann–Whitney rank sum test) but they differed highly significantly with respect to the AP (Figure 4, $p = .006$, same test) and SI (Figure 5, $p < .0001$, same test) distributions. Specifically, the FIT distribution was, overall, more anterior than that of the SAME task (Figure 4), whereas the SAME distribution was more superior to that of the FIT task (Figure 5).

Areas Engaged

Functional activation during task performance was observed in several brain areas. A detailed analysis of the counts and spatial distribution of activated pixels was

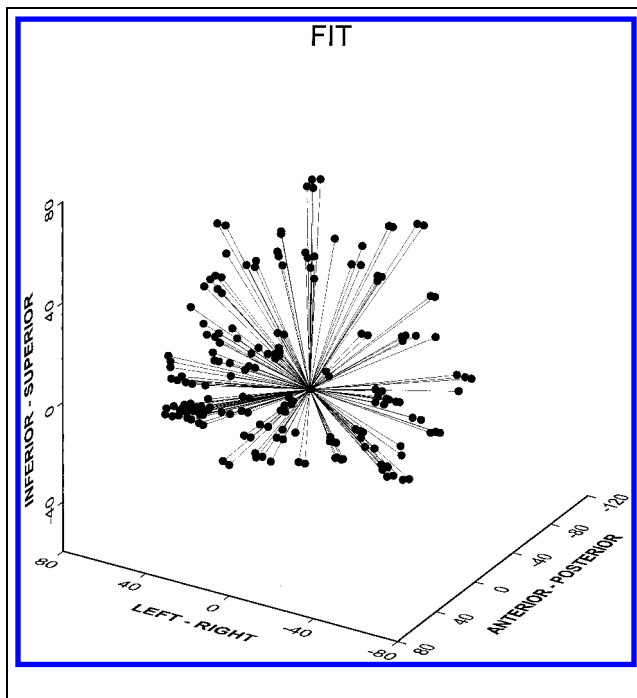


Figure 1. 3-D vectors indicating the Talairach coordinates of activated pixels in the cerebral cortex during the FIT task ($n = 190$).

carried out for those brain areas ($n = 15$, all in the cerebral cortex) in which a consistent activation (in ≥ 3 subjects in at least one task) was observed. Overall, 323 pixels belonged to this category; for the FIT task ($n = 172$), 107 were in the left and 65 in the right hemisphere, whereas for the SAME task ($n = 151$), 87 were in the left

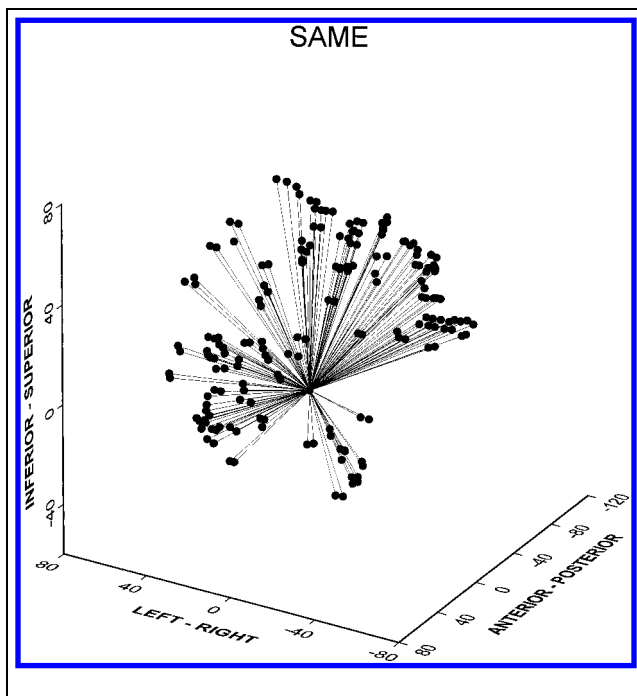


Figure 2. 3-D vectors indicating the Talairach coordinates of activated pixels in the cerebral cortex during the SAME task ($n = 181$).

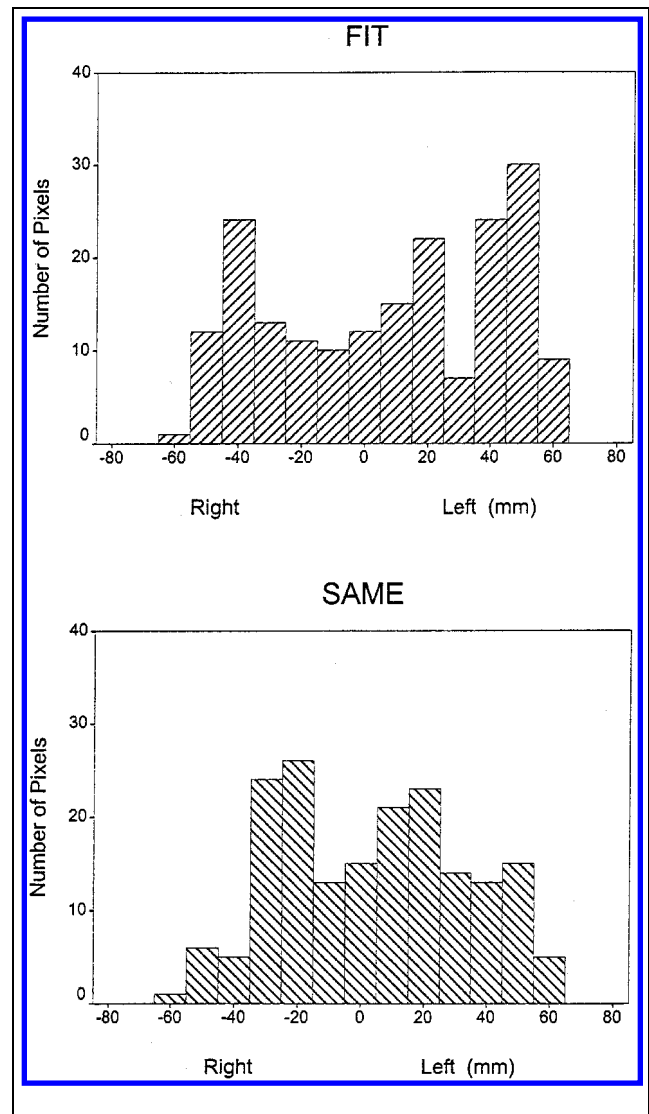


Figure 3. Histograms of left-right distributions of activated pixels, the 3-D coordinates of which are shown in Figures 1 and 2.

and 64 in the right hemisphere. We found the following. With respect to Task (Figure 6), the following areas showed FIT > SAME activation, in decreasing FIT-preference order (bracket indicate ties): GTi, GTs, GC, GFi, GFd, [GTm, GF], GO; this preference was statistically significant for areas GFi, GTi, GTs, GC (in order of decreasing significance level). The following areas showed SAME > FIT activation, in decreasing SAME-preference order: GOi, LPs, Sca, GPrC, GPoC, [GFs, GFm]; this preference was statistically significant for areas GOi, LPs (test for binomial proportion). With respect to Side (Figure 7), areas GPoC, GF, and GO showed equal activation in the left and right hemispheres. The following areas showed a left-hemispheric preference, in decreasing left-preference order: GTs, [GC, LPs], GTi, GTm, GFs, GPrC, GFd, GFi; this preference was statistically significant for areas GTs, LPs, GFs, GC. The following areas showed a right-hemi-

spheric preference, in decreasing right-preference order: Sca, GOi, GFm; however, no such preference was statistically significant. Finally, with respect to Gender (Figure 8), area LPs showed equal activation in women and men. The following areas showed a Women > Men activation, in decreasing women-preference order: GPrC, GOi, GO, GTs, GFs; this preference was statistically significant for areas GPrC and GOi. The following areas showed a Men > Women preference, in decreasing men-preference order: GFi, GC, GF, GTm, Sca, GPoC, GTi, [GFd, GFm]; this preference was statistically significant for areas GFi, GC, GF.

Distribution of Activation Within Specific Areas: General

This analysis was aimed to determine whether the spatial distributions of activated pixels within specific

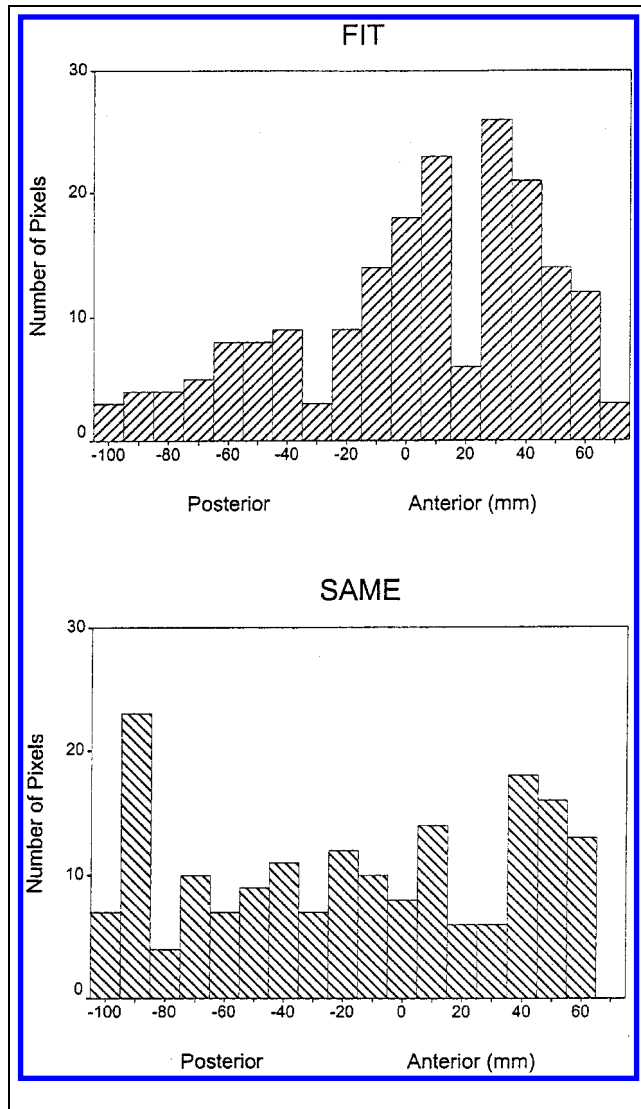


Figure 4. Histograms of anterior–posterior distributions of activated pixels, the 3-D coordinates of which are shown in Figures 1 and 2.

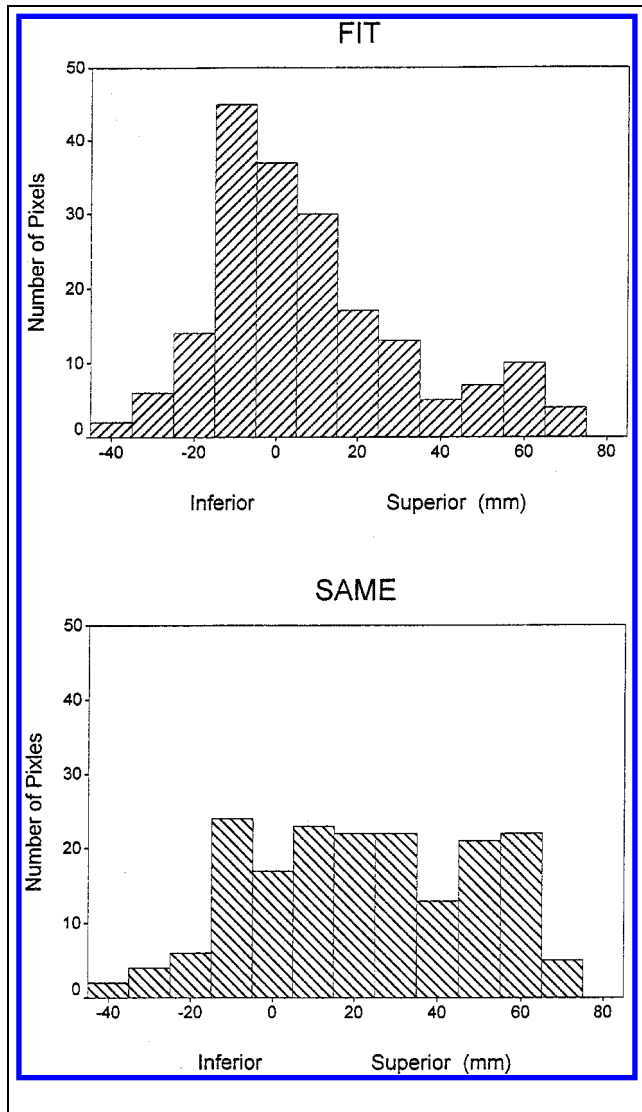


Figure 5. Histograms of superior–inferior distributions of activated pixels, the 3-D coordinates of which are shown in Figures 1 and 2.

areas differed significantly between the two tasks. For that purpose, the Talairach coordinate distributions were compared first all together in three dimensions using multivariate Hotelling’s T^2 ; if this test was significant ($p < .05$), data in each dimension were also tested separately using the Mann–Whitney rank sum test. We accepted factor effects as significant only if both Hotelling’s T^2 and at least one of the three Mann–Whitney tests were significant. These tests were carried out between tasks for the left and right hemispheres, and between hemispheres for each task. We found the following.

Task Differences in Left and Right Hemispheres

With respect to the left hemisphere, the following areas did not differ significantly between the two tasks: GC, GFs, GFm, GFi, GPrC, GTs, GO. The following areas showed significant differences (significantly different dimensions in parentheses): GFd (AP, SI), GPoC (AP),

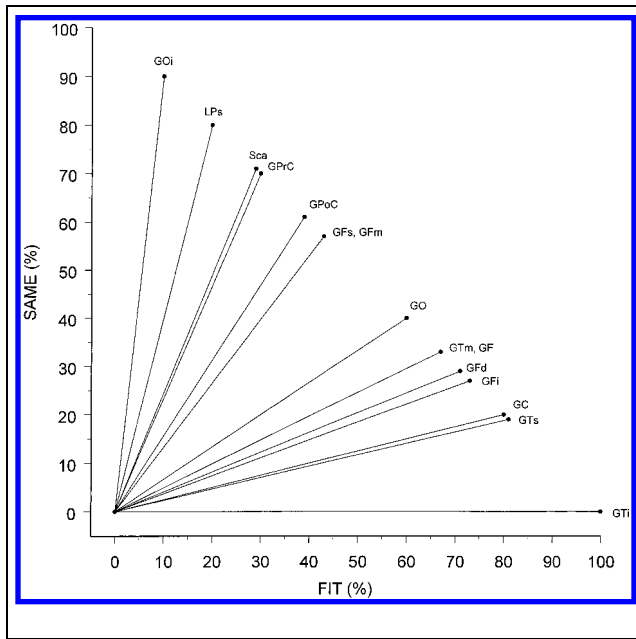


Figure 6. Percent of pixels activated in the FIT and the SAME tasks for each of the 15 areas that showed consistent activation.

GTm (AP, SI), GF (AP). Of the three dimensions, mediolateral (ML) did not differ significantly in any area; AP differed significantly in all areas; and SI differed significantly only in GFd and GTm. Finally, areas Lps (SAME), GTi (FIT), Goi (SAME), and Sca (SAME) were not tested because their activation was confined to one task only, indicated in parentheses.

With respect to the right hemisphere, the following areas did not differ significantly between the two tasks:

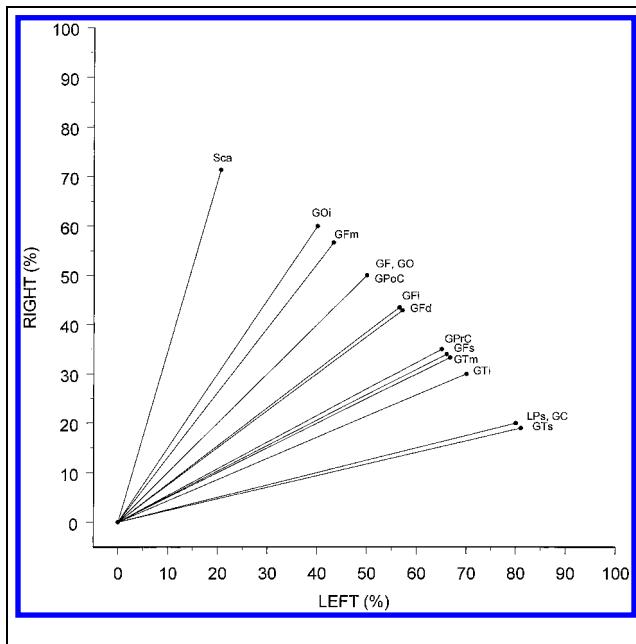


Figure 7. Percent of pixels activated in the left and right hemisphere for each of the 15 areas that showed consistent activation.

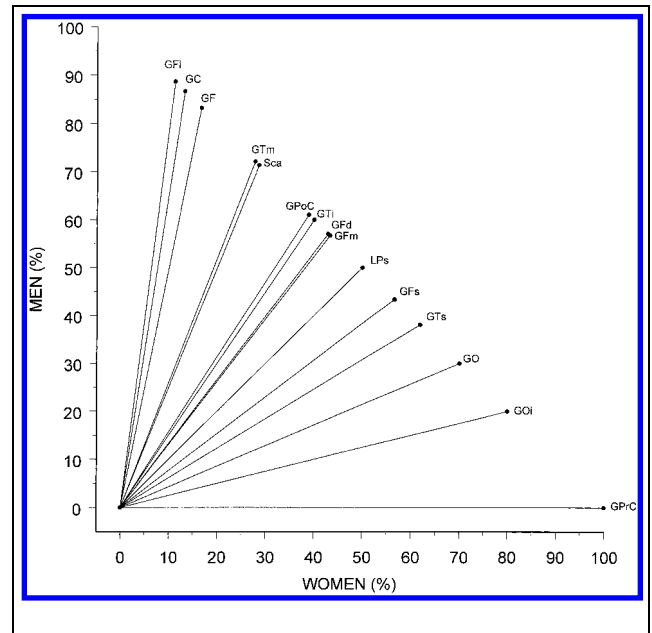


Figure 8. Percent of pixels activated in women and men for each of the 15 areas that showed consistent activation (see text).

GFm, GFs, GPoC, Goi. The following areas showed significant differences: GFi (ML, SI), GPrC (SI), Lps (SI), GF (ML, AP, SI), GO (ML, AP, SI), Sca (AP, SI). Finally, areas GC, GFd, GTs, GTm, and GTi were not tested because their activation was confined only to the FIT task.

Hemisphere Differences in the Two Tasks

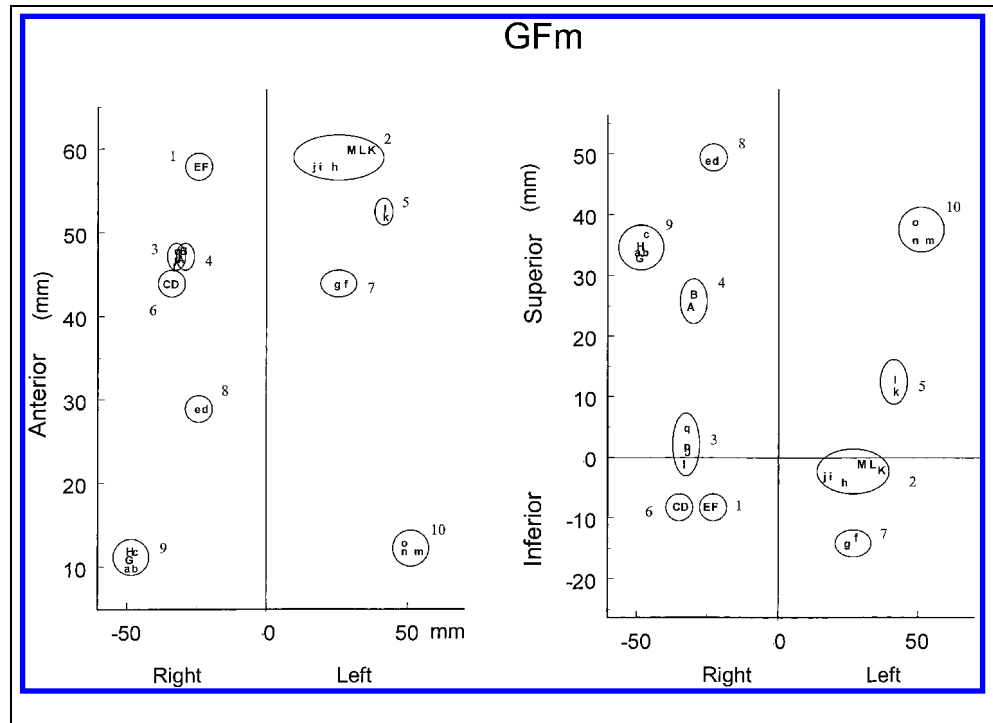
With respect to the FIT task, the following areas did not differ significantly between the two hemispheres: GFd, GFs, GPrC, GTs, GTm. The following areas showed significant differences: GC (SI), GFm (AP), GFi (AP, SI), GTi (ML, AP, SI), GF (ML, AP, SI), GO (ML, AP, SI). Finally, areas GPoC (left), Lps (left), Goi (right), and Sca (right) were not tested because their activation was confined to one hemisphere (in parentheses) only.

With respect to the SAME task, the following areas did not differ significantly between the two hemispheres: GFd, GFi, GFm, GPrC, GPoC, GO, Goi. The following areas showed significant differences: GFs (AP, SI), Lps (SI), GF (ML, AP), Sca (ML, AP, SI). Finally, areas GC (left), GTs (left), GTm (left) were not tested because their activation was confined to one hemisphere (in parentheses) only; GTi was not active in this task at all.

Spatial Distribution of Activation Within Specific Areas: Pixel Clustering

It was of interest to determine the extent to which activated pixels were clustered within specific areas, for two main reasons; first, to examine with a finer grain regions activated, and second, to find out whether activation related to a specific task in an anatomically

Figure 9. Clusters of activated pixels in GfM. Individual pixels are labeled by letters; upper and lower case letters indicate pixels activated in the FIT or SAME tasks, respectively. Identified clusters are numbered and shown in two Talairach coordinate planes.



defined area was localized or widespread. For that purpose, we plotted the coordinates of the activated pixels in the Talairach planes and evaluated their spatial distribution for each area (A, anterior; P, posterior; M, medial; L, lateral; S, superior; I, inferior). Three kinds of clusters were distinguished, namely, (1) clusters composed of pixels activated exclusively during the FIT task (FIT-only clusters), (2) clusters composed of pixels activated exclusively during the SAME task (SAME-only clusters), and (3) clusters composed of pixels some of which were activated during the FIT task and some during the SAME task (FIT + SAME clusters). An example is shown in Figure 9. The overall pixel composition of these clusters is shown in Figure 10. We found the following.

GC

There was a widespread activation in this gyrus that extended from A44 to A11 (i.e., for 33 mm in the AP dimension) and from S4 to I11 (i.e., for 15 mm in the SI dimension). Activation during the FIT task was observed in both hemispheres whereas activation during the SAME task was confined to the left hemisphere. Of seven clusters in total, six were FIT-only (one in the left and five in the right hemisphere) and one FIT + SAME (in the left hemisphere).

Gfd

There was a widespread activation in this gyrus that extended from A54 to P10 (i.e., for 64 mm in the AP

dimension) and from S61 to I13 (i.e., for 74 mm in the SI dimension). Similarly to GC, activation during the FIT task was observed in both hemispheres whereas activation during the SAME task was confined to the left hemisphere but, unlike GC, there were no FIT + SAME clusters. Of four clusters in total, three were FIT-only (one in the left and two in the right hemisphere) and one SAME-only (in the left hemisphere).

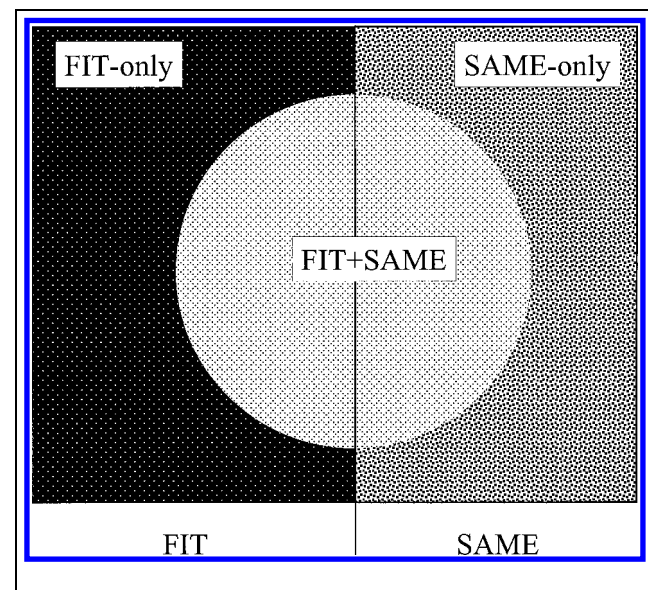


Figure 10. Venn diagrams indicating the number of pixels in FIT-only, SAME-only, and FIT + SAME clusters. Areas are proportional to the counts.

GFs

There was a widespread activation in this gyrus that extended from A64 to P17 (i.e., for 81 mm in the AP dimension), from S63 to S4 (i.e., for 59 mm in the SI dimension), from 2 to 25 in the mediolateral (ML) dimension in the left hemisphere, and from L1 to L25 in the ML dimension in the right hemisphere. Activation in both tasks was observed in both hemispheres. Of 12 clusters in total, 4 were SAME-only, 4 were FIT-only, and 4 were FIT + SAME. All three kinds of clusters were distributed in both hemispheres and along all three dimensions.

GFm (Figure 10)

There was a widespread activation in this gyrus that extended from A60 to P10 (i.e., for 70 mm in the AP dimension), from S49 to I14 (i.e., for 63 mm in the SI dimension), from L17 to L54 in the mediolateral (ML) dimension in the left hemisphere, and from L22 to L50 in the ML dimension in the right hemisphere. Activation in both tasks was observed in both hemispheres. Of 11 clusters in total, 5 were SAME-only, 3 were FIT-only, and 3 were FIT + SAME. All three kinds of clusters were distributed in both hemispheres and along all three dimensions.

GFi

There was a widespread activation in this gyrus that extended from A65 to A8 (i.e., for 57 mm in the AP dimension), from S26 to I18 (i.e., for 44 mm in the SI dimension), from L18 to L54 in the ML dimension in the left hemisphere, and from L17 to L49 in the ML dimension in the right hemisphere. Activation in both tasks was observed in both hemispheres. Of 10 clusters in total, 3 were SAME-only (two in the left and one in the right hemisphere), 5 were FIT-only (three in the left and two in the right hemisphere), and 2 were FIT + SAME (one in the left and one in the right hemisphere).

GPrC

There was a widespread activation in this gyrus that extended from A6 to P20 (i.e., for 26 mm in the AP dimension) and from S65 to S3 (i.e., for 62 mm in the SI dimension). The ML distribution was very restricted in the left hemisphere (within 11 mm, from L38 to L49), but was wider in the right hemisphere (within 45 mm, from L13 to L58). Activation in both tasks was observed in both hemispheres. Of 10 clusters in total, 5 were SAME-only (two in the left and three in the right hemisphere), 3 were FIT-only (two in the left and one in the right hemisphere), and 2 were FIT + SAME (both in the left hemisphere).

GPoC

There was a widespread activation in this gyrus that extended from P16 to P45 (i.e., for 29 mm in the AP dimension) and from S70 to S28 (i.e., for 42 mm in the SI dimension). The ML distribution was similarly extensive in both hemispheres, within 41 mm in the left hemisphere (from L15 to L56), and within 32 mm in the right hemisphere (from L19 to L51). Activation in both tasks was observed in both hemispheres. Of five clusters in total, three were SAME-only (one in the left and two in the right hemisphere), two were FIT-only (in the left hemisphere). No cluster comprised both SAME- and FIT-related pixels.

LPs

The activation in this area was related mostly to the SAME task. The activation extended from P38 to P71 (i.e., for 33 mm in the AP dimension) and from S66 to S33 (i.e., for 33 mm in the SI dimension). The ML distribution was of the same extent in both hemispheres, within 24 mm in the left (from L12 to L36) and the right hemisphere (from L14 to L38). Activation in the left hemisphere was associated with the SAME task, whereas activation in the right hemisphere was observed in both tasks. Of eight clusters in total, six were SAME-only (four in the left and two in the right hemisphere) and two were FIT-only; no clusters were observed comprising both SAME and FIT pixels.

GTs

The activation in this area related mostly to the FIT task. The activation extended from A14 to P37 (i.e., for 23 mm in the AP dimension) and from S18 to I14 (i.e., for 32 mm in the SI dimension). The ML distribution was wider in the left (within 19 mm, from L43 to L62) than the right hemisphere (within 4 mm, from L48 to L52). Activation in the left hemisphere was observed in both tasks, whereas activation in the right hemisphere was associated only with the FIT task. Of seven clusters in total, five were FIT-only (three in the left and two in the right hemisphere) and two were FIT + SAME; no clusters were observed comprising only SAME pixels.

GTm

There was a widespread activation related to both tasks, although predominantly to the FIT task. The activation extended from A5 to P66 (i.e., for 61 mm in the AP dimension) and from S14 to I38 (i.e., for 52 mm in the SI dimension). The ML distribution was of very similar extent in both hemispheres, namely within 21 mm (from L37 to L58) in the left and 19 mm (from L37 to L56) in the right hemisphere. Activation in the left hemisphere was observed in both tasks, whereas activation in the

right hemisphere was associated only with the FIT task. Of eight clusters in total, two were SAME-only (both in the left hemisphere) and six were FIT-only (three in the left and three in the right hemisphere); no clusters were observed comprising both SAME- and FIT-activated pixels.

GTi

All the activation in this area was related only to the FIT task. The activation extended from P2 to P65 (i.e., within 63 mm in the AP dimension) and from I5 to I28 (i.e., within 23 mm in the SI dimension). The ML extent of the activation was 14 mm (from L40 to L54) in the left and 3 mm (from L34 to L37) in the right hemisphere. Of five clusters in total, four were in the left and one in the right hemisphere.

GF

Activation in both tasks was observed in both hemispheres. It extended from P10 to P98 (i.e., within 88 mm in the AP dimension) and from S5 to I31 (i.e., within 26 mm in the SI direction). The ML extent of the activation was 14 mm (from L32 to L46) in the left and 21 mm (from L18 to L39) in the right hemisphere. Of five clusters in total, one was SAME-only (in the right hemisphere), two were FIT-only (both in the right hemisphere), and one was FIT + SAME (in the left hemisphere).

GO

There were three clusters in this area, one of each type. The FIT + SAME cluster was in the left hemisphere and extended from P96 to P99, from S20 to S14, and from L10 to L13. The SAME-only cluster was in the right hemisphere (cluster center coordinates: P95.5, S18.5, L10.5), and the FIT-only cluster was also in the right hemisphere but more anterior (cluster center coordinates: P71, I6, L41.7).

GOi

This area contained mostly SAME-related pixels. Of seven clusters in total, three were located in the left and four in the right hemisphere. The three clusters in the left hemisphere were all SAME-only and spread within 21 mm in the AP dimension (from P75 to P96), 30 mm in the SI dimension (from S22 to I8), and 21 mm in the ML dimension (from L20 to L41). In contrast, the four clusters in the right hemisphere were confined to a more narrow AP and SI distribution; namely, within 6 mm in the AP dimension (from P88 to P94), 14 mm in the SI dimension (from S16 to S2), and 22 mm in the ML dimension (from L16 to L38). Of these four clusters, three were SAME-only and one was FIT + SAME.

Sca

There were three clusters in this area. The single cluster in the left hemisphere was SAME-only (cluster center coordinates: P61, S5, L4). In the right hemisphere, one cluster was SAME-only (cluster center coordinates: P90.7, S15.3, L14.7) and the other was FIT-only (cluster center coordinates: P65, S7.5, L18.5)

Analysis of Clusters of Activated Pixels

Although the overall counts of activated pixels were analyzed above with respect to the side of activation, a separate analysis of their clusters is of interest for these clusters carry additional information concerning the exclusive, or joint, involvement of a cluster in the tasks performed. Table 1 shows the numbers of the clusters of the three categories above for each cortical area analyzed (see preceding section). With respect to brain side, there were very similar number of FIT-only ($n = 44$) and SAME-only ($n = 45$) clusters in the left and right hemispheres. In contrast, there was a substantial lateralization with a left-side preponderance for the FIT + SAME clusters ($n = 12$ and 5 for left and right hemispheres, respectively). These results indicate that the processes that are common to the two tasks are strongly left-

Table 1. Number of the Three Types of Clusters of Activated Pixels (SAME-Only, FIT-Only, FIT + SAME) in Cortical Areas

Area	Cluster						Total
	SAME-Only		FIT-Only		FIT + SAME		
	Left	Right	Left	Right	Left	Right	
GC	0	0	1	5	1	0	7
GFd	1	0	1	2	0	0	4
GFs	2	3	3	1	3	1	13
GFm	3	2	0	3	1	2	11
GFi	1	1	4	2	1	1	10
GPrC	2	3	2	1	2	0	10
GPoC	1	2	2	0	0	0	5
LPs	4	2	0	2	0	0	8
GTs	0	0	3	2	2	0	7
GTm	3	0	3	3	0	0	9
GTi	0	0	4	1	0	0	5
GF	0	1	0	2	1	0	4
GO	0	1	0	1	1	0	3
GOi	3	3	0	0	0	1	7
Sca	1	1	0	1	0	0	3
Total	21	19	23	26	12	5	106

hemisphere lateralized in contrast to those involved exclusively with each one of the two tasks that engage both hemispheres.

A different point concerns the number of distinct areas in which the identified clusters were located. The FIT-only distribution was right-side selective ($n = 9$ and 13 areas in the left and right hemispheres, respectively), whereas the SAME-only distributions was evenly distributed ($n = 10$ areas) between left and right side. Both of them differed from the FIT + SAME distribution, which remained left-lateralized ($n = 8$ and 4 areas in the left and right hemispheres, respectively).

Analysis of Pixels in Specific Cluster Types

The analyses above were applied to the numbers of the three types of clusters of activated pixels. In this section, we analyze the numbers of pixels contained in these clusters because a cluster can contain different numbers of pixels. Specifically we sought to assess task selectivity, lateralization and gender difference for particular areas, as well as possible associations between these factors.

Task Selectivity

We analyzed task selectivity by focusing on the pixels contained within the FIT-only and SAME-only clusters. Figure 11 plots the percentage of pixels in each one of these cluster types for each cortical area shown as a vector from the origin of the task axes. Task selectivity is assessed as a continuous, quantitative function by the angle of a brain area vector from a task axis. For

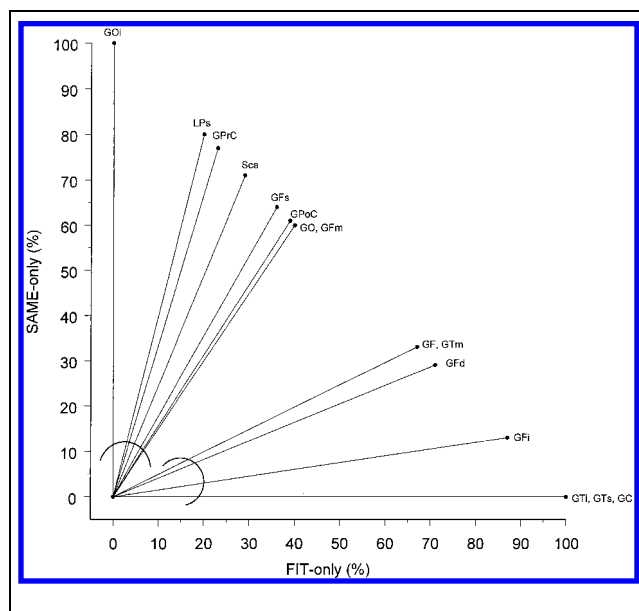


Figure 11. Percent of pixels contained in FIT-only and SAME-only clusters for each of the 15 areas that showed consistent activation.

example, if the angle is measured counterclockwise from the FIT axis, a value of $< 45^\circ$ would indicate FIT selectivity, with smaller angles denoting higher selectivity; and similarly for SAME selectivity assessed by angles measured clockwise from the SAME task axis. It can be seen that there were two distinct groups of areas near the task axes, indicating task selectivity. The FIT-selective areas ($n = 7$) comprised (in order of decreasing selectivity) GTs, GTi, GC, GFi, GFd, GF, and GTm, whereas the SAME-selective areas ($n = 8$) comprised GOi, LPs, GPrC, Sca, GFs, GPoC, GFm and GO. These results suggest that there is a graded selectivity of the various areas with respect to the tasks used. The FIT-selective areas comprised all the temporal lobe areas, the two frontal areas in the medial wall and the inferior frontal gyrus. By contrast, the SAME-selective areas comprised all the occipital areas and a contiguous sheet of areas on the lateral surface extending from the superior and middle frontal gyrus to the superior parietal lobule.

It is apparent from the analyses above that the relative involvement of an area in each of the two tasks used can be assessed in two different ways, as shown in Figures 6 and 11. One way is to regard all the pixels irrespective of cluster membership (Figure 6) whereas the other is to regard only the pixels contained in the task-selective clusters (Figure 11). It can be seen in these two figures that the relative task selectivity of each area was very congruent between the two cases; in fact, only GO changed from being more FIT-selective in the overall case (Figure 6) to being SAME-selective in the task-clustering case (Figure 11), and in both cases the task selectivity of this area was rather weak as its vector was near the 45-degree diagonal.

Side Selectivity

Side selectivity was assessed by analyzing the counts of pixels contained in each cluster type with respect to their location in the left and right hemisphere. We found the following. (a) There were 97 pixels in the SAME-only clusters, of which 48 were in the left and 49 in the right hemisphere (Figure 12, upper left panel); there was no statistically significant effect of Side ($p = .66$, t test on L/R log ratios, $n = 8$ subjects). (b) There were 111 pixels in the FIT-only clusters, of which 49 were in the left and 62 in the right hemisphere (Figure 12, upper right panel); there was no statistically significant effect of Side ($p = .61$, t test on L/R log ratios, $n = 8$ subjects). Finally, (c) there were 115 pixels in the FIT + SAME clusters, of which 87 were in the left and 28 in the right hemisphere (Figure 12, lower panel); this left-hemispheric preponderance was statistically significant ($p = .0265$, t test on L/R log ratios, $n = 8$ subjects).

In summary, there was equal left-right distribution for the SAME-only pixels, a slight right-side preponderance for the FIT-only pixels, and a substantial left-side pre-

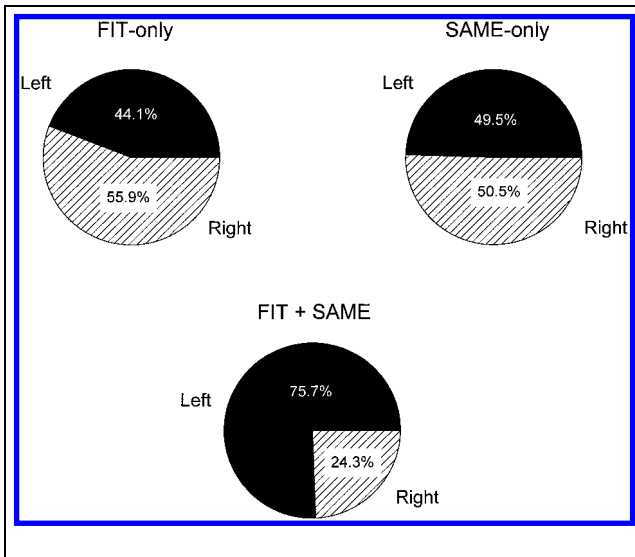


Figure 12. Percentages of activated pixels in the left and right hemisphere for the FIT-only, SAME-only, and FIT + SAME clusters.

ponderance for the FIT + SAME pixels. These results indicate that the processes that are common to the tasks used involve predominantly the left hemisphere, whereas those processes more specific to the individual tasks involve both the left and the right hemisphere.

Gender-Side Association

The analyses above showed a basic difference in the laterality of activated pixels contained in specific cluster types (Figure 12). Specifically, there was an approximately equal distribution of pixels contained in FIT-only and SAME-only clusters in the two hemispheres but a definite left hemisphere preponderance for pixels contained within FIT + SAME clusters. It would be interesting to know whether there exist differences between the two genders with respect to the laterality of these activations. For that purpose, we counted the number of activated pixels for each gender within each cluster type. The results are illustrated in Figure 13. It can be seen

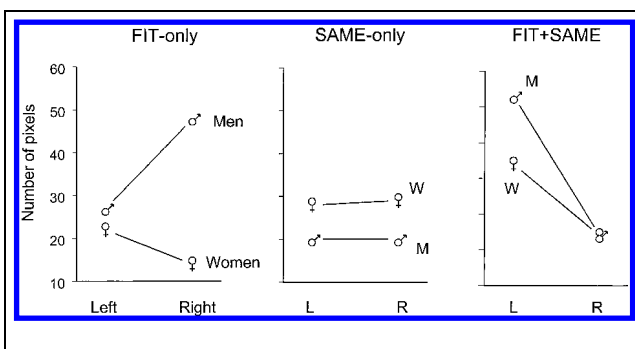


Figure 13. Numbers of activated pixels in women and men for the FIT-only, SAME-only, and FIT+SAME clusters.

that there were substantial differences in the left/right hemispheric distribution between women and men, depending on the type of cluster. Specifically, for the FIT-only clusters (Figure 13, left), there was a clear right-hemisphere preponderance for men [$n(\text{right}) = 48$, $n(\text{left}) = 27$ pixels] and a left-hemisphere preponderance for women [$n(\text{left}) = 22$, $n(\text{right}) = 14$ pixels]. In fact, every single man (but no woman) showed the right-hemisphere preponderance whereas three out of four women showed a left-hemisphere preponderance and one woman had an equal number of pixels in the left and right hemispheres. The statistical significance of this hemispheric lateralization between the two genders was assessed as follows. For each subject, the R/L ratio was calculated and was log-transformed to normalize its distribution; then a two-group t test was performed on these log ratios to evaluate the effect of gender. Indeed, this effect was statistically highly significant ($p = .01$, t test, $n = 8$, i.e., four subjects per gender group). The mean log ratios and their SEM are shown in Figure 14. Finally, we calculated the average normalized signal change (See Methods) across activated pixels for each subject and performed the same analysis as above on their R/L log ratios. There was no statistically significant effect of gender on these R/L log ratios ($p = .89$, t test, $n = 8$, i.e., four subjects per gender group). This finding indicates that the gender differences lie in the extent and not the intensity of activation.

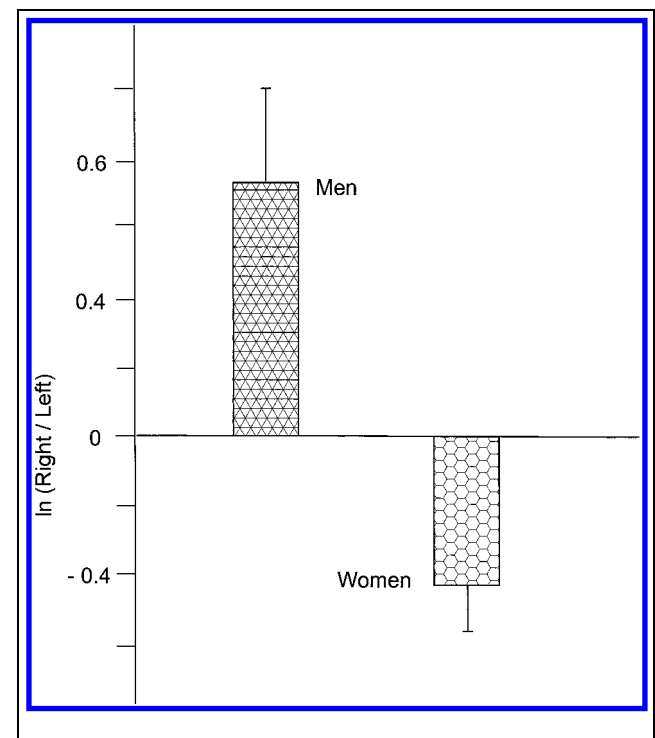


Figure 14. Mean \pm SEM of right/left log ratios of activated pixels contained in FIT-only clusters in men and women; these values differed statistically significantly (see text). The data correspond to those depicted in Figure 13, left.

In contrast to this lateralization pattern between women and men in the FIT-only case, there was a practically equal left–right distribution for both genders in the SAME-only case [Figure 13, middle; Men: $n(\text{right}) = n(\text{left}) = 20$; Women: $n(\text{right}) = 29$, $n(\text{left}) = 28$]. There was no statistically significant effect of the gender either on the counts R/L log ratios ($p = .61$, t test, $n = 8$, i.e., four subjects per gender group) or the pixel normalized signal change ($p = .53$, t test).

Finally, with respect to the FIT + SAME case, an almost equal number of pixels was activated in the right hemisphere in women and men but the number of pixels in the left hemisphere was higher in men than in women [Figure 13, right; Men: $n(14) = n(\text{left}) = 53$; Women: $n(\text{right}) = 14$, $n(\text{left}) = 34$]. There was no statistically significant effect of the gender either on the counts R/L log ratios ($p = .11$, t test, $n = 8$, i.e., four subjects per gender group) or the pixel normalized signal change ($p = .34$, t test).

Differential Involvement of Areas in Task-Specific Clusters Between Women and Men

The results above were based on an analysis of counts of activated pixels and demonstrated significant differences in lateralization between women and men in FIT-only and SAME-only clusters. A different question concerns the localization of the activated pixels. This issue was investigated at two levels. First, the 3-D distributions of the Talairach coordinates were compared between genders for each cluster-type/hemisphere combination. We found that these distributions differed statistically highly significantly only in one case, namely the FIT-only/Right hemisphere combination ($p = .001$, multivariate Hotelling's T^2 test). A more detailed evaluation of the differences between these two distributions was obtained by analyzing their component distributions in the three coordinate planes. The two genders did not differ significantly with respect to the mediolateral ($p = .75$, Mann–Whitney rank sum test) or the anteroposterior dimension ($p = .89$, same test) but they differed highly significantly with respect to the superior/inferior dimension ($p = .0035$, same test). Specifically, the distribution of FIT-only pixels in the right hemisphere was much more inferior for men (average: inferior 3.02, Talairach coordinate) than for women (average: superior 20.36). With respect to the areas involved, the following areas were activated in both genders: GFd, GC, GFm, LPs, GTs, GTm; areas GFs and GPrC were activated only in women, whereas GFi, GTi, GF, GO, Sca were activated only in men.

Common Clusters

We found the following concerning the pixels contained in the FIT + SAME clusters with respect to area and side of activation. First, the following areas did not contain

such clusters: GFd, GPoC, LPs, GTm, GTi, Sca. Second, the lateral frontal areas GFs, GFm and GFi had the highest number of pixels contained in the FIT + SAME clusters and accounted, collectively, for $78/115 = 68\%$ of total. Finally, of the eight areas that contained such clusters (GC, GFs, GFm, GFi, GPrC, GTs, GF, GO), all but GFm showed a left hemispheric preponderance.

Activation in Other Areas

The following areas were activated inconsistently, in <3 subjects (number of subjects in parentheses): PCu (2), GL (2), IPS (2), Gob (2), Gh (2), INS (2), LPi (1), Uncus (1), GOm (1), GOs (1), Cu (1), Lpc (1), Spo (1), internal segment of globus pallidus (2), and cerebellum (1).

DISCUSSION

The overall objectives of this study were to analyze the brain activation patterns underlying two different tasks of visual image processing, namely visual object construction and shape discrimination. We found that brain activation was distributed across several areas, most consistently in the cerebral cortex. Some activations were task-specific, whereas others were common to both tasks. With respect to brain areas, there was a gradation of task selectivity as well as a gradation in the hemispheric lateralization of the activation. Since the presentation of stimuli was not confined to a particular visual hemifield, presumably both hemispheres were available for information processing. Finally, women and men differed significantly in the degree of involvement of the right hemisphere in the visual construction task, which was much greater in men than in women. We discuss each one of these findings separately below.

Methodological Considerations

Although a detailed analysis of the spatial distributions of the activated pixels within specific regions was a major goal of the study, other approaches in analyzing fMRI signals have been used in studies with different objectives. For example, the average signal in regions of interest (ROIs) has been used to analyze the relations between the intensity of the fMRI signal and behavioral variables in a task. Apparently, different methods are appropriate for different experimental goals, and there is no unique way to cover all possible objectives. The use of integrated ROI signals has the advantage that no threshold considerations enter the analysis but at the cost that a possibly spatially restricted change may be diluted by the averaging. This method also has the advantage of providing a continuous variable that is well suited for a variety of statistical analyses, including all classical techniques, such as analysis of variance, regression, tests of equality of means, etc. In contrast, the identification of activated pixels relies on the application

of a threshold that can be somewhat arbitrary. In return, one gains a detailed spatial distribution of the foci of activation, which can provide important information concerning, e.g., possible specialized areas within a region. In addition to classical statistical methods, other methods appropriate for spatial point distributions are applicable here, including cluster analysis.

In the present study we focused on the spatial distribution of activated pixels. We used very conservative criteria for labeling a given pixel as “activated” including a signal change of at least 3 *SD*, a coefficient of variation of $\leq 2\%$ in the control task, and a spatial contiguity criterion. Each activated pixel was taken to indicate a clear focus of activation. The data thus obtained were then analyzed within two different frameworks. In one, the activated pixels for the two tasks were analyzed independently of each other, that is within the general framework of investigating the brain mechanisms underlying visual shape discrimination irrespective of the mechanisms underlying visual object construction. For example, these same analyses would have been performed if just one task had been used, and they are valid within that context. They comprised general analyses of the counts of activated pixels and their overall spatial distribution in the brain. More specifically, the effects of, and the relations between, the factors of Task, Side, and Gender were assessed, and the involvement of various brain areas was evaluated. The effects of these factors was also assessed separately for each area; given that areas may differ in size, which was not calculated in this study, no across-areas comparisons were performed.

The second framework of analysis concerned the detailed spatial distribution of the activated pixels in each area taking into account the conjunction, so to speak, of the two tasks. Essentially, the distributions from the two tasks were superimposed and the resulting joint distributions analyzed in terms of pixel clustering. This analysis afforded the identification of regions containing closely spaced activated pixels from both tasks, a fact that we interpreted as indicating involvement in common processes underlying the two tasks used. The effects of various factors were then assessed on these newly defined subsets of activated pixels.

Activation Patterns in Visual Object Construction and Visual Shape Discrimination

Performance of both tasks resulted in widespread cortical activation in both hemispheres. This is in accord with neuropsychological studies that have shown that visuo-perceptual, visuospatial, and visuoconstructive deficits can result from focal lesions in various cortical areas (Mehta, Newcombe, & Damasio, 1987; Black & Bernard, 1984; Kertesz & Dubrowolski, 1981). The analysis based on clustering provided more specific information, in that there were striking differences in the overall activation patterns of the two tasks with respect to sidedness and

gender (Figures 13, 14). This is even more interesting, since the total number of activated pixels was very similar in the two tasks. Given that the two tasks involved the same visual stimuli (fragments of a square) as well as the same visual control stimuli (whole square), the results above document fundamental differences in the brain mechanisms underlying each task as well as basic differences between women and men in the visual object construction task.

The effects of sidedness and gender on the performance of visual tasks have been studied previously in patients with brain damage. However, such studies have been focused on visuoconstructive abilities, best reflected in our FIT task, in addition to studies of language-related functions. In fact, most studies have contrasted these two kinds of functions with respect to laterality and gender whereas, to our knowledge, there has not been any study of the influence of these factors on simple visual shape discrimination uncontaminated by factors impinging on visual “expertise” (e.g., face recognition), complex-shape discrimination, mental rotation, spatial location, or memory loads, to name but a few. With respect to lateralization of visuoconstructive function, it is generally believed that the right hemisphere plays a crucial role in that function (Mack & Levine, 1981; Nebes, 1978; Gott, 1973; Smith, 1969; Benton, 1967; Piercy, Hécaen, & Ajuriaguerra, 1960). However, there is substantial controversy regarding this matter (see Gainotti, 1985; De Renzi, 1982). Part of this controversy stems from the fact that differences may exist between women and men such that the effects of right or left hemispheric lesions may depend on gender. With respect to men, right hemispheric lesions seem to be more effective in producing visuoconstructive deficits, as compared to either left-hemispheric lesions in men or right hemispheric lesions in women (Lewis & Kamptner, 1987; McGlone & Kertesz, 1973). With respect to women, the effects of left hemispheric lesions on visuoconstructive functions are similar to those of right hemispheric lesions in women (Lewis & Kamptner, 1987; McGlone & Kertesz, 1973) but similar (McGlone & Kertesz, 1973) or worse (Lewis & Kamptner, 1987) than left hemispheric lesions in men. Assuming a preponderant role of the right and left hemispheres in visuoconstructive and language skills, respectively, it has been proposed that a given task may be performed using spatial or verbal procedures, and that women, being more expert in language skills (Meyer & Bentig, 1961; Wechsel, 1958; Hobson, 1947) may tend to use preferentially verbal strategies (Kimura, 1969), hence their smaller dependence on the right hemisphere. Then, the gender differences are explained by postulating that men and women employ fundamentally different strategies to perform these tasks based on spatial or verbal operations, respectively. A variant of this idea makes use of the concept of “synthetic” (non verbal) and “analytic” (verbal) functions for which the right and left

hemispheres are specialized, respectively (Levy, 1969). Specifically, it has been proposed that tasks involving perceptual synthesis rely on the right hemisphere (in men), whereas tasks involving perceptual analysis or language skills rely on the left hemisphere (in women) (Tucker, 1976). The argument, then, can be formulated as follows: men tend to use spatial/synthetic strategies, hence their right-hemisphere preponderance in solving visuoconstructive problems; in contrast, women tend to employ verbal/analytic strategies, hence their left hemispheric preponderance. Although this is a plausible scheme with reasonable support, it nevertheless includes a fair amount of speculation. What seems to be especially weak is the supposed reliance of women on verbal strategies in solving visuoconstructive tasks. Although this could be the case for fairly complex tasks, it does not seem plausible for simple ones. And, specifically, it would seem difficult to believe that a piecemeal, analytic, verbal strategy would be the strategy employed to perform our FIT task in which the individual visual stimuli were simple line drawings and the “whole” figure was the highly common square. Therefore, it is hard to attribute the apparent left hemispheric preponderance in women to the use of verbal strategies. We believe that, for our data, the crucial observation is not so much a preponderance of the left hemisphere as a substantial decrease in the involvement of the right hemisphere in women is in performing the FIT task. Indeed, there was hardly any difference between men and women with regard to left hemispheric activation, whereas there was a major difference in the involvement of the right hemisphere that was much more extensively activated in men than in women with regard to specific, FIT-only pixels (Figures 13, 14). Given that verbal strategies may not be plausible in our case, and assuming that right hemispheric activation truly underlies visuoconstructive operations, it seems as if women are much more efficient in using their right hemisphere than men, hence the reduced extent of activation of that hemisphere.

Areas Engaged

The discussion above revolved around the grand picture of overall hemispheric activation. We discuss next the potentially differential involvement of specific brain areas. As mentioned above, the experimental design in these studies was such that the visual stimuli were identical during both the control and the task periods but the judgements, and, therefore, the underlying processes, differed since one involved a visual discrimination of two fragments of a square (SAME task) whereas the other involved a visual construction by assessing the fit-ness of pairs of fragments to make a complete square (FIT task). It is noteworthy that the overall number of activated pixels was very similar in the two tasks (Table 1). Therefore, any differences between

the two tasks should be in the distributions of the activated pixels, that is, in the pattern of activation of various brain areas. We found that these patterns partially overlapped; namely, there were brain areas activated only (or mostly) in one or the other task, but several others were activated in both tasks although at different degrees of specificity. These findings are in accord with the fact that the same visual information (i.e., the same fragments) was processed in both tasks, although for different purposes (i.e., discrimination or construction). We discuss below first the differential involvement of various areas in the two tasks and then compare them to extract common and specific components of brain processing in visual discrimination and construction.

The cluster analysis of the 15 consistently activated cortical areas ($n = 151$ pixels) revealed that 10 areas in the left and 10 in the right hemisphere comprised clusters composed exclusively of SAME-only activated pixels (21 clusters in the left and 19 in the right hemisphere; Table 1). These areas were in all cortical lobes, which indicates that visual shape discrimination involves widely distributed neural substrates. Specifically, the SAME-selective areas comprised occipital areas (Sca, GOi) and a number of contiguous areas in a fronto-parietal sheet extending from the superior and middle frontal gyri to the superior parietal lobule (GFs, GFm, GPrC, GPoC, LPs). With respect to the FIT task, 9 areas in the left and 13 in right hemisphere, distributed over all major lobes, comprised clusters composed exclusively of FIT-only activated pixels (23 clusters in the left and 26 in the right hemisphere; Table 1). These areas were in all cortical lobes and comprised all temporal areas (GTs, GTm, GTi, GF), the two frontal areas in the medial wall (GC, GFd) and the inferior frontal gyrus (GFi). Thus, the brain activation patterns differed substantially between the two tasks, which presumably reflects different processes involved. Finally, several areas contained FIT + SAME clusters (Table 1). It is reasonable to suppose that these areas are related to processes common to both tasks including early stages of visual image processing and late stages of decision making since both tasks involved the same visual images as input and binary responses as output. It is interesting that the following areas did not contain any FIT+SAME clusters: GFd, GPoC, LPs, GTm, GTi, Sca.

Owen, Milner, Petrides, and Evans (1996) studied the brain activation patterns related to memory for object features using positron emission tomography (PET). By performing subtraction analyses they identified areas related to encoding and/or retrieving of object features and object location. They found that the following areas were involved in the encoding of object features: GR/Gob, GFi, GF (in the left hemisphere) and GR/Gob, GFi, GFd, GOi/GF, Sca (in the right hemisphere), whereas the following areas were involved in retrieving stimulus

features: GF_i, GF, GT_i/GF, Sca, GO (in the left hemisphere) and GF_i, GT_i/GF, GT_i, GF/GO_i, Sca (in the right hemisphere). [These areas were defined using the Talairach coordinates provided in Owen et al. (1996) and the Talairach and Tournoux (1988) atlas.] Since processing of stimulus features is likely to be an important aspect in our tasks, these results are relevant to our findings. Interestingly, of the areas above, all except GR/Gob were consistently activated in our study. (Gob was activated in only two subjects.) It is possible that GR/Gob might be involved in processing complex visual stimuli, since our stimuli were much simpler than those used in the study of Owen et al. (1996). Complex visual objects were also used in the fMRI study by Malach et al. (1995) and were contrasted with textures. Object-related activation was found in lateral occipital cortex with coordinates corresponding to areas GF/GO/GO_i in the Talairach and Tournoux (1988) atlas. These areas were also activated in the present study. In a PET study, Vandenberghe et al. (1996) areas activated more during orientation discrimination of visual stimulus gratings than during stimulus detection. The Talairach coordinates given in Table 3 of Vandenberghe et al. (1996) correspond to the following cortical areas in the Talairach and Tournoux (1988) atlas: GF, GF/GO, LPs/PCu, GC, GFs/GF_m, GPrC. All of these areas were consistently activated in our tasks, except PCu that was activated in only two subjects.

A different issue concerns mental image generation. This question was investigated recently using fMRI (D'Esposito et al., 1997). Subjects listened to words and were instructed to generate visual mental images of the words' referents. A reliable and robust activation of left GT_i was observed. It is interesting that GT_i was also clearly activated in the present study with a left-hemispheric preponderance (Figure 7) and a unique selectivity for the FIT task (Figures 6, 11). Since the FIT (but not the SAME) task involved a judgement on a mentally constructed object (i.e., the square), it is tempting to suppose that the activation of GT_i we observed provides evidence for a mental image generation of this object in the FIT task. It is noteworthy that in the right-hemisphere distribution of FIT-only clusters GT_i (together with GF, GF_i, GO, and Sca) were exclusively activated in men. This points to a potentially different strategy by which women and men solved the FIT task.

Task Processing Dimensions

Behavioral tasks are accomplished by employing a series of processes that, in turn, are carried out in several dimensions. A central issue in behavioral neuroscience is to identify the brain mechanisms that are involved in a specific task with respect to the corresponding processes and their components. There is apparently a continuum of complexity in these do-

main, from simple tasks composed of a few and/or low-dimensional processes to complex tasks consisting of many and/or high-dimensional processes. With respect to brain mechanisms, the trade-off is that simple tasks may be more easily understood but at the price of a limited understanding of the broader mechanisms, whereas complex tasks address these broader mechanisms but at the price of a less thorough understanding. The quantification of task complexity is a difficult issue that has not been resolved adequately. As alluded to above, the number of processes involved and the number of dimensions along which they operate could serve as approximations for the description of a task in this domain. There are several ways by which one can gain an insight into the processing dimensions in a given task with respect to brain processing (see, e.g., Tagaris, Strupp, Andersen Uğurbil, & Georgopoulos, 1997; Tagaris et al., 1998; Friston, Frith, Fletcher, Liddle, & Frackowiak, 1996; Snyder & Harris, 1993; Boles, 1991, 1996; Samar, 1983). In a recent paper (Whang, Crowe, & Georgopoulos, 1999) we used multi-dimensional scaling (MDS) to analyze response times obtained in two tasks that were similar to those employed in the present study. Analyses of the response times observed for pairs of objects in the SAME and FIT tasks identified two different primary dimensions along which objects were distributed in the MDS stimulus configuration space; namely, enclosure of space (i.e., how many orthogonal turns were contained in a shape) for the SAME task and symmetry (i.e., presence of symmetry along the horizontal or vertical axis, diagonally, or both) for the FIT task. Moreover, analyses of the response times using classical analyses of variance further validated the significance of these differential effects of the two dimensions (Whang et al., 1999).

There are several ways by which a correct judgement can be arrived at in these tasks. For example, in the SAME task, two geometrical shapes have to be judged as to whether they are the same or not. Apparently, a correct judgement that two shapes are different can be reached by comparing the entire shapes or only parts of them, and, in the latter case, the process can stop at the first detection of a difference. And similarly, a correct judgement that two shapes are the same can be the result of a global "entire shape" comparison or the result of an exhaustive comparison of each and every segment of the two shapes, where all segments are judged to be "not different." In all cases, a common process seems to be that of comparing elemental or aggregate segments between the two visual shapes. The results of the MDS analysis above (Whang et al., 1999) of the response times suggest that such comparisons seem to be carried out predominantly along the enclosure dimension above, and the essence of this dimension can be reduced to the number of angles in a shape that, in turn, can be thought to refer to the number of changes in orientation of segments.

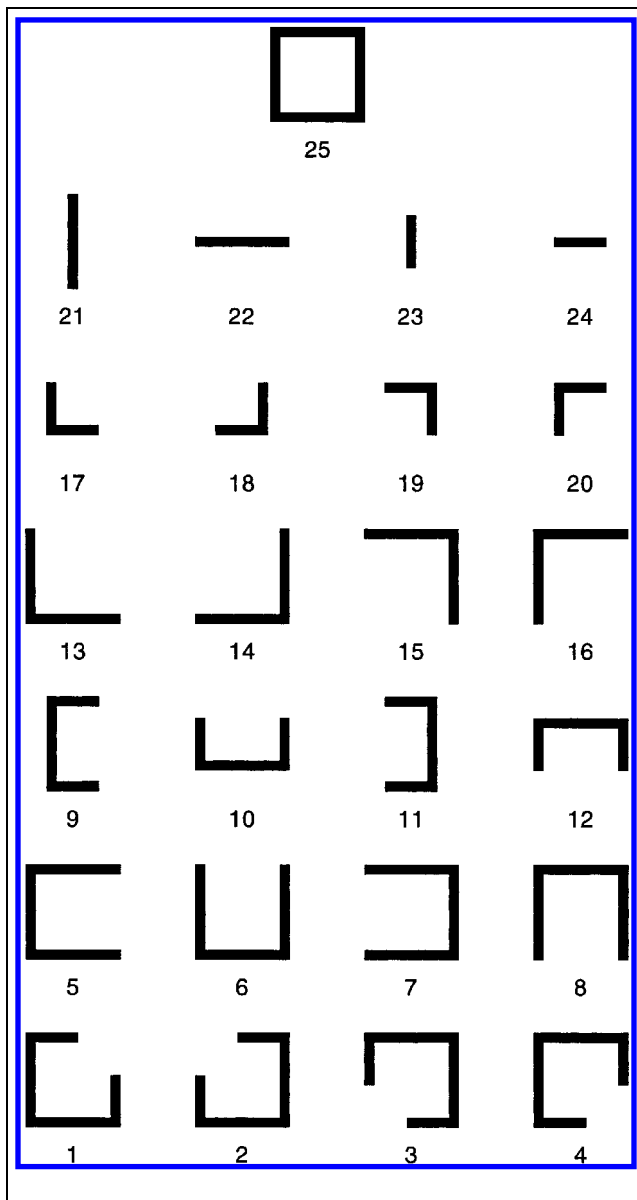


Figure 15. The 25 fragments of the square used.

In contrast to the above considerations, the main process in the FIT task seems to operate on the symmetry aspect of the shapes (Whang et al., 1999). This is a more complex aspect of an object because it involves an *axis* with respect to which symmetry is judged. Thus, whereas enclosure can be determined from the object alone, symmetry implies a reference to a frame external to the objects. Consequently, the comparison of objects with respect to the enclosure can be performed by relying on the visual image of the object whereas the comparison with respect to their symmetry requires the definition of an axis to be compared, which is an additional, derived, second-order measure. Therefore, it is not surprising that the response times in the FIT task were consistently higher than those in the SAME task (see Figure 6 in Whang et al., 1999).

Seen in the light of the discussion above, our results would suggest that the overall SAME- and FIT-selective activation patterns observed might reflect the dimensions of object enclosure and symmetry, respectively. Unfortunately, these are fairly broad dimensions, and there has been no systematic investigation of this problem. Although the present experiments provide interesting possibilities, these are only points of departure for future studies in which these dimensions could be varied quantitatively in separate blocks of trials so that the resulting brain activation patterns could be compared accordingly.

METHODS

Subjects

Eight healthy, right-handed human subjects [four women and four men, age (mean \pm *SD*) 30.1 \pm 9.0 and 31.5 \pm 5.5 years, respectively] participated in these experiments as paid volunteers. The study protocol was approved by the University of Minnesota Institutional Review Board and informed consent was signed by each subject.

Behavioral Tasks

The subjects performed two experimental tasks and one control task. Pairs of objects were picked randomly from a set of 25 oriented objects, consisting of 24 oriented fragments of a square and a complete square (Figure 15). Pairs were presented to the subjects approximately every 3 sec. In the visual shape discrimination task (SAME task, Figure 16), subjects had to compare the two fragments and indicate, by pushing one of two buttons, whether they were identical or not. In the visual object construction task (FIT task, Figure 16), subjects had to decide whether the two fragments could match to form a perfect square. In both tasks, the subjects were instructed not to rotate the fragments in

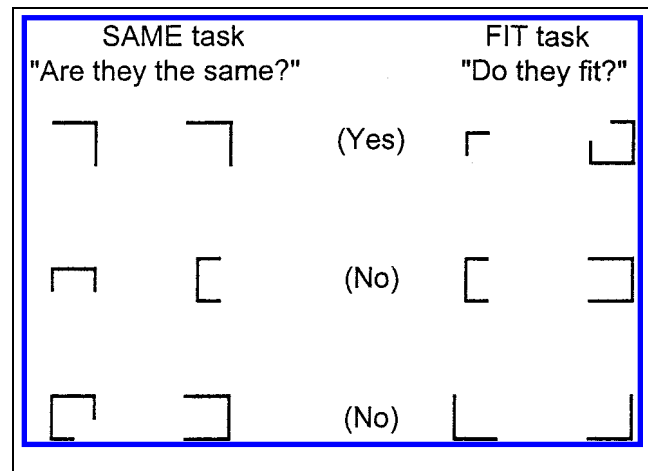


Figure 16. Schematic diagram illustrating the tasks used.

making their decision. Finally, in the control task, a single square was presented at the same rate and subjects pushed any of the two keys at random.

Each one of the two experimental tasks described above was performed during the “task period” that was preceded and followed by a “control period” during which the control task was performed. For a subject, the two tasks were presented in a randomized block design and the subject performed just the three blocks above.

fMRI

A 4-tesla whole body system with head gradients and a homogeneous RF coil (SIS, Sunnyvale, CA/Siemens, Erlangen, Germany) was used. A head-support system with several foam pads was used to minimize head movements during the experiment. Multislice coronal anatomic images (T_1 -weighted) were obtained using a turbo-FLASH sequence with 5-mm slice thickness and in-plane spatial resolution of $1.88 \times 1.88 \text{ mm}^2$. For functional imaging, a T_2^* -weighted, single-shot echo-planar imaging (EPI) sequence was employed ($TE = 25 \text{ msec}$). Imaging planes were coronal, with 5-mm slice thickness and in-plane spatial resolution of $3.75 \times 3.75 \text{ mm}^2$. In total, 35–39 slices were collected, covering the whole brain. The acquisition time for a single slice was 30 msec; for a complete multislice image, the repetition time was typically 5.0 sec. Images were collected continuously during the experiment. The duration of each of the two experiments was 9.7–10.3 min. In total, 124 multislice images were collected in each experiment (40, 60, and 24 images during the first control, the task, and the second control period, respectively). The fMRI analysis package STIMULATE (version 5.7, Center for Magnetic Resonance Research, University of Minnesota Medical School, Minneapolis, MN) was used to process the fMRI images. All images were screened for motion artifacts and images were rejected if artifacts were present.

Data Analysis

General

Standard statistical methods (Snedecor & Cochran, 1967), were used to display and analyze the data. Counts of activated pixels were log-transformed before subjected to statistical analyses. The statistical significance of the factors of Task, Side, and Gender, and their interactions, was assessed using a subject-by-subject repeated measures analysis of variance in which Gender was a grouping factor and Task and Side were repeated-measures factors with nesting of Side within Task, since images of both hemispheres were acquired simultaneously for a given task. The SPSS (SPSS, Chicago, IL, 1993) and BMDP/Dynamic (BMDP Statistical Software, Los Angeles, CA, 1992) were used for these analyses.

fMRI Data

The raw data were log-transformed and detrended. The logarithmic transformation was dictated by the fact that the increase of the fMRI signal during the task period was proportional to the baseline of the preceding control period (Figure 17), which indicates a proportional model. The detrending was necessitated by the presence of time trends; control and task periods were detrended separately following the log transformation.

Functional activation maps were generated by comparing the average intensity of each pixel during the task period to that observed during the first control period. A given pixel was deemed to be “activated” based on a conservative combination of criteria. (a) For each pixel the coefficient of variation for the first control period had to be no greater than 2%; (b) pixel contiguity was required (see below); and (c) an average cluster z score value in the signal change (see below) of 3 or higher was required. The criterion for the coefficient of variation was used because it has been documented that the coefficient of variation is higher in the vicinity of large vessels as well as outside the brain (Kim, Hendrich, Hu, Merkle, & Uğurbil, 1991). The z score values were calculated as follows. First, the mean signal (across images) during the first control (C) and the task (T) periods were calculated. Second, a normalized signal change (S) was computed as: $S = (T - C)/C$. Third, the mean (S_{MEAN}) and SD of positive S in all pixels lying in the brain of a given subject were calculated separately for the FIT and SAME tasks. Fourth, the value of $S_{\text{MEAN}} + 3SD$ (i.e., z score = 3) was calculated. Finally, the pixel contiguity criterion required the presence of at least two contiguous pixels in the same plane sharing at least a full side and an average z score of ≥ 3 . Specific clusters were identified using qualitative inspection of the data plotted in Talairach axes pairwise and the BMDP K-means

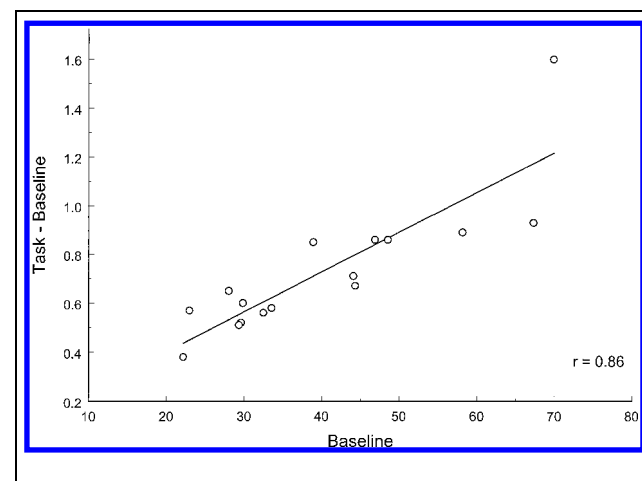


Figure 17. The difference between the fMRI signal during the task period from that of the preceding control period (baseline) is plotted against the latter (arbitrary units). Points are differences of averages of all pixels in the brain ($n = 8 \text{ subjects} \times 2 \text{ tasks} = 16 \text{ averages}$).

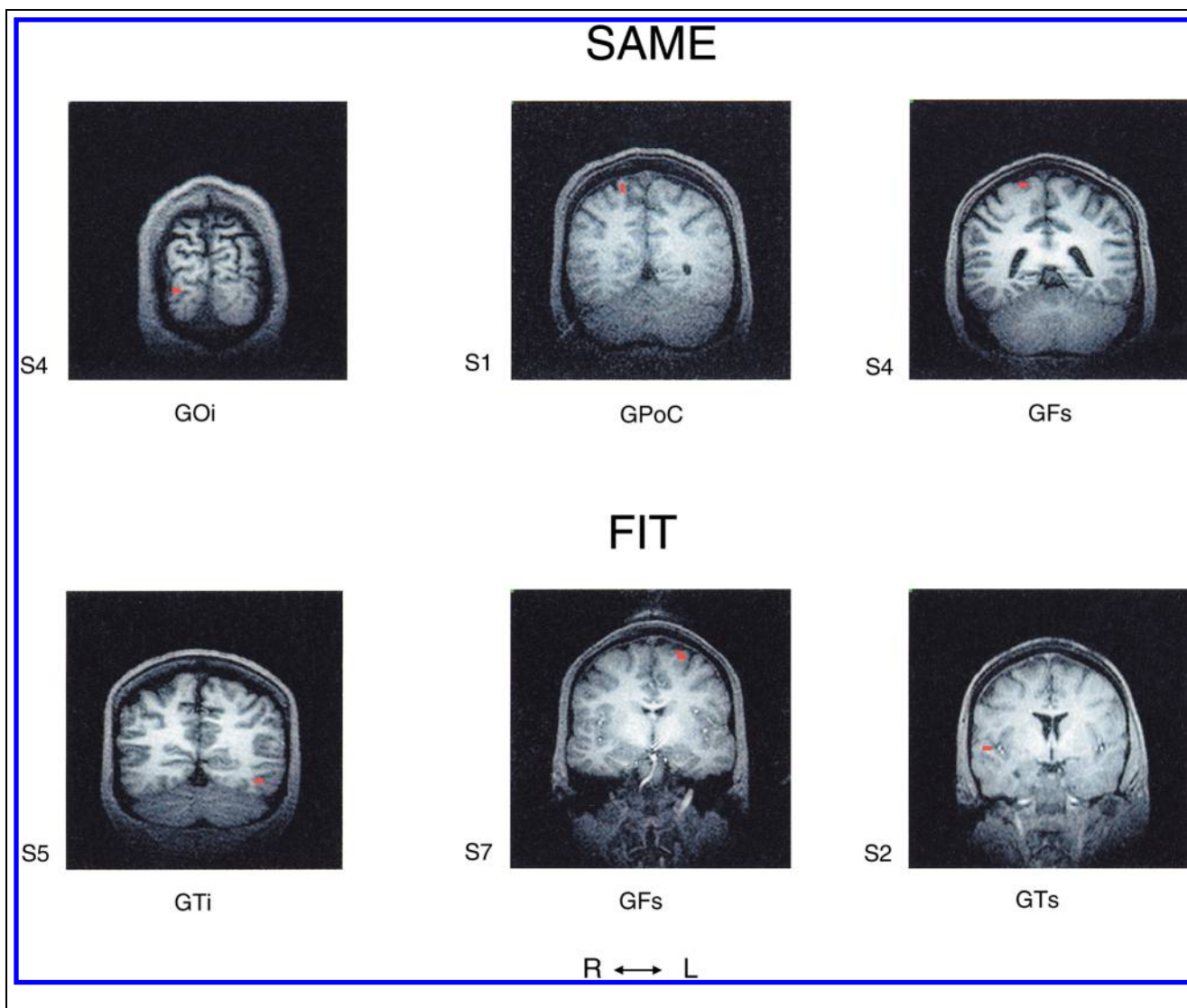


Figure 18. Examples of functional activation maps from single subjects. (The notation to the left of each map indicates the subject.) There are two pixels per map; the Talairach coordinates (in brackets) of the center of the activation and the average z scores are as follows, from left to right. SAME: S4: $[-27, -90, 5]$, $z = 3.55$; S1: $[-19, -38, 63]$, $z = 3.953$; S4: $[-15, -13, 63]$, $z = 4.356$; FIT: S5: $[44, -65, -5]$, $z = 6.156$; S7: $[21, 13, 49]$, $z = 4.076$; S2: $[-48, -3, -2]$, $z = 5.694$.

clustering program. Examples of functional activation maps from single subjects are shown in Figure 18.

Assignment to Brain Areas

The assignment of activated pixels to specific regions was based on Talairach coordinates and anatomical landmarks. The following abbreviations from the Talairach and Tournoux (1988) atlas are used in the paper: GFs, gyrus frontalis superior; GFm, gyrus frontalis medius; GFi, gyrus frontalis inferior; GC, gyrus cinguli; GOB, gyrus orbitalis, GFd, gyrus frontalis medialis; GPrC, gyrus precentralis; GPoC, gyrus postcentralis; LPs, lobulus parietalis superior; LPi, lobulus parietalis inferior; IPS, intraparietal sulcus (our notation); INS, insula; Lpc, lobulus paracentralis; SPO, sulcus parieto-

occipitalis; GTs, gyrus temporalis superior; GTm, gyrus temporalis medius; GTi, gyrus temporalis inferior; GF, gyrus fusiformis; GL, gyrus lingualis; Sca, sulcus calcarinus; GO, gyrus occipitalis; GOM, gyrus occipitalis medius; GOi, gyrus occipitalis inferior; Cu, cuneus; Pcu, precuneus.

Acknowledgments

This study was supported by United States Public Health Service grants NS32919 and RR088079, the United States Department of Veterans Affairs, and the American Legion Chair in Brain Sciences. We thank Mr. David Crowe for help with the experiment and Dr. Scott Lewis for assisting with data display.

Reprint requests should be sent to: Dr. Apostolos P. Georgopoulos, Brain Sciences Center (11B), VAMC, One Veterans Drive, Minneapolis, MN 55417, USA.

REFERENCES

- Benton, A. L. (1967). Constructional apraxia and the minor hemisphere. *Confinia Neurologica*, *29*, 1–16.
- Black, F. W., & Bernard, B. A. (1984). Constructional apraxia as a function of lesion locus and size in patients with focal brain damage. *Cortex*, *20*, 111–120.
- Boles, D. B. (1991). Factor analysis and the cerebral hemispheres: Pilot study and parietal functions. *Neuropsychologia*, *29*, 59–91.
- Boles, D. B. (1996). Factor analysis and the cerebral hemispheres: “Unlocalized” functions. *Neuropsychologia*, *34*, 723–736.
- De Renzi, E. (1982). *Disorders of space exploration and cognition*. Baffins Lane: Wiley.
- D’Esposito, M., Detre, J. A., Aguirre, G. K., Stallcup, M., Alsop, D. C., Tippet, L. J., & Farah, M. J. (1997). A functional MRI study of mental image generation. *Neuropsychologia*, *35*, 725–730.
- Friston, K. J., Frith, C. D., Fletcher, P., Liddle, P. F., & Frackowiak, R. S. (1996). Functional topography: Multidimensional scaling and functional connectivity in the brain. *Cerebral Cortex*, *6*, 156–164.
- Gainotti, G. (1985). Constructional apraxia. In J. A. M. Frederiks (Ed.), *Handbook of clinical neurology* (pp. 491–506). Amsterdam: Elsevier.
- Gott, P. S. (1973). Cognitive abilities following right and left hemispherectomy. *Cortex*, *9*, 266–274.
- Hobson, J. (1947). Sex-differences in primary mental abilities. *Journal of Educational Research*, *41*, 126–132.
- Kertesz, A., & Dubrowolski, S. (1981). Right-hemisphere deficits, lesion size and location. *Journal of Clinical Neuropsychology*, *4*, 283–299.
- Kim, S.-G., Hendrich, K., Hu, X., Merkle, H., & Uğurbil, K. (1991). Potential pitfalls of functional MRI using conventional gradient-recalled echo techniques. *NMR in Biomedicine*, *7*, 69–74.
- Kimura, D. (1969). Spatial localization in the left and right visual fields. *Canadian Journal of Psychology*, *23*, 445–458.
- Levy, J. (1969). Possible basis for the evolution of lateral specialization of the human brain. *Nature*, *224*, 614–615.
- Lewis, R. S., & Kamptner, L. N. L. (1987). Sex differences in spatial task performance of patients with and without unilateral cerebral lesions. *Brain and Cognition*, *6*, 142–152.
- Mack, J. L., & Levine, R. N. (1981). The basis of visual constructional disability in patients with unilateral cerebral lesions. *Cortex*, *17*, 515–532.
- Malach, R., Reppas, J. B., Benson, R. R., Kwong, K. K., Jiang, H., Kennedy, W. A., Ledden, P. J., Brady, T. J., Rosen, B. R., & Tootell, R. B. H. (1995). Object-related activity revealed by functional magnetic resonance imaging in human occipital cortex. *Proceedings of the National Academy of Sciences, U.S.A.*, *92*, 8135–8139.
- McGlone, J., & Kertesz, A. (1973). Sex differences in cerebral processing of visuospatial tasks. *Cortex*, *9*, 313–320.
- Mehta, Z., Newcombe, F., & Damasio, H. (1987). A left hemisphere contribution to visuospatial processing. *Cortex*, *23*, 447–461.
- Meyer, W., & Bentig, A. (1961). A longitudinal study of the primary mental abilities test. *Journal of Educational Psychology*, *52*, 50–60.
- Nebes, R. D. (1978). Direct examination of cognitive function in the right and left hemispheres. In M. Kinsbourne (Ed.), *Asymmetrical function of the brain* (pp. 99–137). Cambridge, UK: Cambridge University Press.
- Owen, A. M., Milner, B., Petrides, M., & Evans, A. C. (1996). Memory for object features versus memory for object location: A positron-emission tomography study of encoding and retrieval processes. *Proceedings of the National Academy of Sciences, U.S.A.*, *93*, 9212–9217.
- Piercy, M., Hécaen, H., & Ajuriaguerra, J. (1960). Constructional apraxia associated with unilateral cerebral lesions. Left and right sided cases compared. *Brain*, *83*, 225–242.
- Samar, V. J. (1983). Multidimensional influences of cerebral asymmetries on visual half-field asymmetries and cognitive skills. *Brain and Cognition*, *2*, 355–382.
- Smith, A. (1969). Nondominant hemispherectomy. *Neurology*, *19*, 167–171.
- Snedecor, G. W., & Cochran, W. G. (1967). *Statistical methods*. 6th ed. Ames, IA: Iowa State University.
- Snyder, P. J., & Harris, L. J. (1993). Handedness, sex, and familial sinistrality effects on spatial tasks. *Cortex*, *29*, 115–134.
- Tagaris, G. A., Richter, W., Kim, S.-G., Pellizzer, G., Andersen, P., Uğurbil, K., & Georgopoulos, A. P. (1998). Functional magnetic resonance imaging of mental rotation and memory scanning: A multidimensional scaling analysis of brain activation patterns. *Brain Research Reviews*, *26*, 106–112.
- Tagaris, G. A., Strupp, J. P., Andersen, P., Uğurbil, K., & Georgopoulos, A. P. (1997). Mental rotation studied by functional magnetic resonance imaging at high field (4 Tesla): Performance and cortical activation. *Journal of Cognitive Neuroscience*, *9*, 419–432.
- Talairach, J., & Tournoux, P. (1988). *Co-planar stereotaxic atlas of the human brain*. New York: Thieme Medical Publishers.
- Tucker, D. M. (1976). Sex differences in hemispheric specialization for synthetic visuospatial functions. *Neuropsychologia*, *14*, 447–454.
- Vandenbergh, R., Dupont, P., De Bruyn, B., Bormans, G., Michiels, J., Mortelmans, L., & Orban, G. A. (1996). The influence of stimulus location on the brain activation pattern in detection and orientation discrimination. A PET study of visual attention. *Brain*, *119*, 1263–1276.
- Wechsler, D. (1958). *Measurement and appraisal of adult intelligence*. 4th ed. Baltimore: Williams & Wilkins.
- Whang, K. C., Crow, D. A., & Georgopoulos, A. P. (1999). Multidimensional scaling analysis of two construction-related tasks. *Experimental Brain Research*, *125*, 231–238.

This article has been cited by:

1. Kristina Küper, Hubert D. Zimmer. 2018. The impact of perceptual changes to studied items on ERP correlates of familiarity and recollection is subject to hemispheric asymmetries. *Brain and Cognition* **122**, 17-25. [[Crossref](#)]
2. И.И. Коробейникова, Н.А. Каратыгин, Е.В. Бирюкова, Я. А. Венерина. 2018. ПРОСТРАНСТВЕННЫЕ ХАРАКТЕРИСТИКИ ТЕТА-РИТМА ЭЭГ И ВРЕМЯ ПЕРЕКЛЮЧЕНИЯ ВНИМАНИЯ В УСЛОВИЯХ ЭКЗОГЕННЫХ ПОМЕХ, "Российский физиологический журнал им. И.М. Сеченова". *Российский физиологический журнал им. И. М. Сеченова* :10, 1215-1226. [[Crossref](#)]
3. A. V. Slavutskaya, N. Yu. Gerasimenko, E. S. Mikhailova. 2014. Mechanisms of orientation sensitivity in the human visual system: Part I. Behavioral characteristics of orientation sensitivity. Influence of the task type, experimental conditions, and gender. *Human Physiology* **40**:6, 660-668. [[Crossref](#)]
4. A. V. Slavutskaya, N. Yu. Gerasimenko, E. S. Mikhailova. 2014. Gender-Related Strategies for Solving Visuospatial Tasks. *Neuroscience and Behavioral Physiology* **44**:6, 709-716. [[Crossref](#)]
5. Jan Scholz, Valentina Tomassini, Heidi Johansen-Berg. Individual Differences in White Matter Microstructure in the Healthy Brain 301-316. [[Crossref](#)]
6. Katya Rubia, Lena Lim, Christine Ecker, Rozmin Halari, Vincent Giampietro, Andrew Simmons, Michael Brammer, Anna Smith. 2013. Effects of age and gender on neural networks of motor response inhibition: From adolescence to mid-adulthood. *NeuroImage* **83**, 690-703. [[Crossref](#)]
7. E.S. Mikhailova, A.V. Slavutskaya, N.Yu. Gerasimenko. 2012. Gender differences in the recognition of spatially transformed figures: Behavioral data and event-related potentials (ERPs). *Neuroscience Letters* **524**:2, 74-78. [[Crossref](#)]
8. A. V. Slavutskaya, N. Yu. Gerasimenko, E. S. Mikhailova. 2012. Recognition of spatially transformed objects in men and women: Analysis of behavior and evoked potentials. *Human Physiology* **38**:3, 238-248. [[Crossref](#)]
9. B. Liu, X. Meng, G. Wu, Y. Huang. 2012. Feature precedence in processing multifeature visual information in the human brain: an event-related potential study. *Neuroscience* **210**, 145-151. [[Crossref](#)]
10. Victoria J. Bourne, Adele M. Maxwell. 2010. Examining the sex difference in lateralisation for processing facial emotion: Does biological sex or psychological gender identity matter?. *Neuropsychologia* **48**:5, 1289-1294. [[Crossref](#)]
11. Aitao Lu, Guiping Xu, Hua Jin, Lei Mo, Jijia Zhang, John X. Zhang. 2010. Electrophysiological evidence for effects of color knowledge in object recognition. *Neuroscience Letters* **469**:3, 405-410. [[Crossref](#)]
12. Anastasia Christakou, Rozmin Halari, Anna B. Smith, Eve Ifkovits, Mick Brammer, Katya Rubia. 2009. Sex-dependent age modulation of frontostriatal and temporo-parietal activation during cognitive control. *NeuroImage* **48**:1, 223-236. [[Crossref](#)]
13. Jan Scholz, Valentina Tomassini, Heidi Johansen-Berg. Individual Differences in White Matter Microstructure in the Healthy Brain 237-249. [[Crossref](#)]
14. Peka S. Christova, Scott M. Lewis, Georgios A. Tagaris, Kâmil Uğurbil, Apostolos P. Georgopoulos. 2008. A voxel-by-voxel parametric fMRI study of motor mental rotation: hemispheric specialization and gender differences in neural processing efficiency. *Experimental Brain Research* **189**:1, 79-90. [[Crossref](#)]
15. Romain Martin, Claude Houssemand, Christine Schiltz, Yves Burnod, Frédéric Alexandre. 2008. Is there continuity between categorical and coordinate spatial relations coding?. *Neuropsychologia* **46**:2, 576-594. [[Crossref](#)]
16. Teresa Jacobson Kimberley, Dana D. Birkholz, Renee A. Hancock, Sarah M. VonBank, Teresa N. Werth. 2008. Reliability of fMRI during a Continuous Motor Task: Assessment of Analysis Techniques. *Journal of Neuroimaging* **18**:1, 18-27. [[Crossref](#)]
17. Teresa Jacobson Kimberley, Scott M Lewis. 2007. Understanding Neuroimaging. *Physical Therapy* **87**:6, 670-683. [[Crossref](#)]
18. Jonathan J. Ratcliff, Arlene I. Greenspan, Felicia C. Goldstein, Anthony Y. Stringer, Tamara Bushnik, Flora M. Hammond, Thomas A. Novack, John Whyte, David W. Wright. 2007. Gender and traumatic brain injury: Do the sexes fare differently?. *Brain Injury* **21**:10, 1023-1030. [[Crossref](#)]
19. Emily C. Bell, Morgan C. Willson, Alan H. Wilman, Sanjay Dave, Peter H. Silverstone. 2006. Males and females differ in brain activation during cognitive tasks. *NeuroImage* **30**:2, 529-538. [[Crossref](#)]
20. M. Pedersen, F.A. Barrios. 2006. Comparison of different statistical analyses in visual stimulus FMRI. *Journal of Neuroradiology* **33**:2, 81-86. [[Crossref](#)]
21. Elke R. Gizewski, Eva Krause, Isabel Wanke, Michael Forsting, Wolfgang Senf. 2006. Gender-specific cerebral activation during cognitive tasks using functional MRI: comparison of women in mid-luteal phase and men. *Neuroradiology* **48**:1, 14-20. [[Crossref](#)]

22. Pavlos Gourtzelidis, Charidimos Tzagarakis, Scott M. Lewis, David A. Crowe, Edward Auerbach, Trenton A. Jerde, Kâmil Uğurbil, Apostolos P. Georgopoulos. 2005. Mental maze solving: directional fMRI tuning and population coding in the superior parietal lobule. *Experimental Brain Research* **165**:3, 273-282. [[Crossref](#)]
23. Scott M. Lewis, Trenton A. Jerde, Charidimos Tzagarakis, Pavlos Gourtzelidis, Maria-Alexandra Georgopoulos, Nikolaos Tsekos, Bagrat Amirikian, Seong-Gi Kim, Kâmil Uğurbil, Apostolos P. Georgopoulos. 2005. Logarithmic transformation for high-field BOLD fMRI data. *Experimental Brain Research* **165**:4, 447-453. [[Crossref](#)]
24. R. W. Van Boven, J. E. Ingeholm, M. S. Beauchamp, P. C. Bickle, L. G. Ungerleider. 2005. Tactile form and location processing in the human brain. *Proceedings of the National Academy of Sciences* **102**:35, 12601-12605. [[Crossref](#)]
25. Emily C. Bell, Morgan C. Willson, Alan H. Wilman, Sanjay Dave, Peter H. Silverstone. 2005. Differential effects of chronic lithium and valproate on brain activation in healthy volunteers. *Human Psychopharmacology: Clinical and Experimental* **20**:6, 415-424. [[Crossref](#)]
26. Victoria J. Bourne. 2005. Lateralised processing of positive facial emotion: sex differences in strength of hemispheric dominance. *Neuropsychologia* **43**:6, 953-956. [[Crossref](#)]
27. J.T. Francis, J.K. Chapin. 2004. Force Field Apparatus for Investigating Movement Control in Small Animals. *IEEE Transactions on Biomedical Engineering* **51**:6, 963-965. [[Crossref](#)]
28. Reinhard Leichner, Marcel Grether. 2004. Funktionelle Hemisphärenasymmetrie im Vergleich der Geschlechter. *Zeitschrift für Psychologie / Journal of Psychology* **212**:2, 76-86. [[Crossref](#)]
29. Alice Mado Proverbio, Fabiana Burco, Marzia del Zotto, Alberto Zani. 2004. Blue piglets? Electrophysiological evidence for the primacy of shape over color in object recognition. *Cognitive Brain Research* **18**:3, 288-300. [[Crossref](#)]
30. D Pins, M.E Meyer, J Foucher, G Humphreys, M Boucart. 2004. Neural correlates of implicit object identification. *Neuropsychologia* **42**:9, 1247-1259. [[Crossref](#)]
31. Marlene Behrmann, Ruth Kimchi. 2003. What does visual agnosia tell us about perceptual organization and its relationship to object perception?. *Journal of Experimental Psychology: Human Perception and Performance* **29**:1, 19-42. [[Crossref](#)]
32. Alice Mado Proverbio, Alberto Zani. Visual Selective Attention to Object Features 275-VII. [[Crossref](#)]
33. Alice Mado Proverbio, Paola Esposito, Alberto Zani. 2002. Early involvement of the temporal area in attentional selection of grating orientation: an ERP study. *Cognitive Brain Research* **13**:1, 139-151. [[Crossref](#)]
34. Markus Ullsperger, D. Yves von Cramon, Notger G. Müller. 2002. Interactions of focal cortical lesions with error processing: Evidence from event-related brain potentials. *Neuropsychology* **16**:4, 548-561. [[Crossref](#)]
35. 2001. Current Awareness. *NMR in Biomedicine* **14**:3, 217-222. [[Crossref](#)]
36. M. Reske, U. Habel. Geschlechts- und alters abhängige Effekte 177-185. [[Crossref](#)]